pubs.acs.org/acschemicalbiology

Articles

Cellular Labeling of Phosphatidylserine Using Clickable Serine Probes

Christelle F. Ancajas, Shahrina Alam, Daiane S. Alves, Yue Zhou, Nicholas M. Wadsworth, Chelsi D. Cassilly, Tanei J. Ricks, Adam J. Carr, Todd B. Reynolds, Francisco N. Barrera, and Michael D. Best*

Cite This: *ACS Chem. Biol.* 2023, 18, 377−384

Read Online

ACCESS | Metrics & More | Article Recommendations | Supporting Information

ABSTRACT: Phosphatidylserine (PS) is a key lipid that plays important roles in disease-related biological processes, and therefore, the means to track PS in live cells are invaluable. Herein, we describe the metabolic labeling of PS in *Saccharomyces cerevisiae* cells using analogues of serine, a PS precursor, derivatized with azide moieties at either the amino (**N**-L-**SerN$_3$**) or carbonyl (**C**-L-**SerN$_3$**) groups. The conservative click tag modification enabled these compounds to infiltrate normal lipid biosynthetic pathways, thereby producing tagged PS molecules as supported by mass spectrometry studies, thin-layer chromatography (TLC) analysis, and further derivatization with fluorescent reporters via click chemistry to enable imaging in yeast cells. This approach shows strong prospects for elucidating the complex biosynthetic and trafficking pathways involving PS.

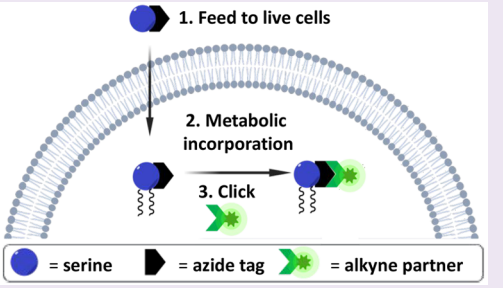

INTRODUCTION

Lipids control many critical biological pathways, and therefore, aberrant lipid biosynthesis and activity commonly correlate with diseases, including cancer.[1−4] Phosphatidylserine (PS) is an important biomarker that participates in diverse biological processes. PS acts as a ligand for a number of proteins, thereby driving their membrane association through noncovalent protein−lipid binding interactions.[5] A well-studied example involves Annexin A5,[6] which is a protein that responds to PS membrane translocation and is involved in key anticoagulation events,[7,8] antiphospholipid antibody syndrome,[9,10] and has been used for cancer imaging applications.[11] The latter application arises since, under normal conditions, PS is primarily localized within the inner leaflet of the plasma membrane but is translocated to the outer leaflet during processes including capacitation of sperm cells,[12] apoptosis,[13−15] and in certain cancers.[15,16] As such, PS can serve as an effective biomarker for tumors.

Despite the significance of lipids such as PS, the ability to track the biosynthesis and transport of lipid molecules *in vivo* remains a substantial challenge because of the complexity of lipid biosynthetic pathways. The abundance and subcellular localization of lipids are tightly controlled through complex biosynthetic and trafficking networks, including vesicle- and protein-mediated transfer, and defects in any of these processes typically result in disease.[17−22] While PS biosynthesis can occur through a variety of pathways depending on the organism, these processes generally exploit serine as a substrate for an exchange reaction with a lipid. For example, yeast convert cytidine diphosphate-diacylglycerol (CDP-DAG) and serine into PS and cytidine monophosphate (CMP) (Figure S1), while mammalian cells instead utilize serine for trans-phosphatidylation of phosphatidylcholine (PC) or phosphatidylethanolamine (PE). Another pathway for PS production involves the acylation of lyso-phosphatidylserine (LPS), a lysolipid that has also garnered interest for involvement in biological events including inflammatory processes.[23] PS can be converted back to these precursors through deacylation to LPS or through decarboxylation to PE followed by methylation to PC.

Studies employing tagged biosynthetic precursors are invaluable for the dynamic detection and characterization of complex biomolecules in cells. This approach has been enhanced by introducing diminutive clickable tags onto substrates, which provides analogues that successfully infiltrate biosynthetic pathways and generate functionalized products in cells.[24,25] Pioneering work in this field focused on labeling complex cell-surface glycans using sugar precursor analogues bearing clickable tags.[26−30] Since then, this precursor labeling strategy has been shown to be valuable for analyzing other biomolecules, such as lipid metabolic targets. While much of the seminal work has involved tagged fatty acids (FAs) for tracking lipid metabolism[31] and studying posttranslational

Received: October 28, 2022
Accepted: January 25, 2023
Published: February 6, 2023

https://doi.org/10.1021/acschembio.2c00813
ACS Chem. Biol. 2023, 18, 377−384

Scheme 1. Schematic for the Labeling of Lipid Products and Detection by Mass Spectrometry (A), as Well as Fluorescence Microscopy Imaging Using Clickable Cy3-DBCO (B) and TLC Imaging via Copper-Catalyzed Azide−alkyne Cycloaddition (CuAAC) (C), with a Scale bar = 5 μm

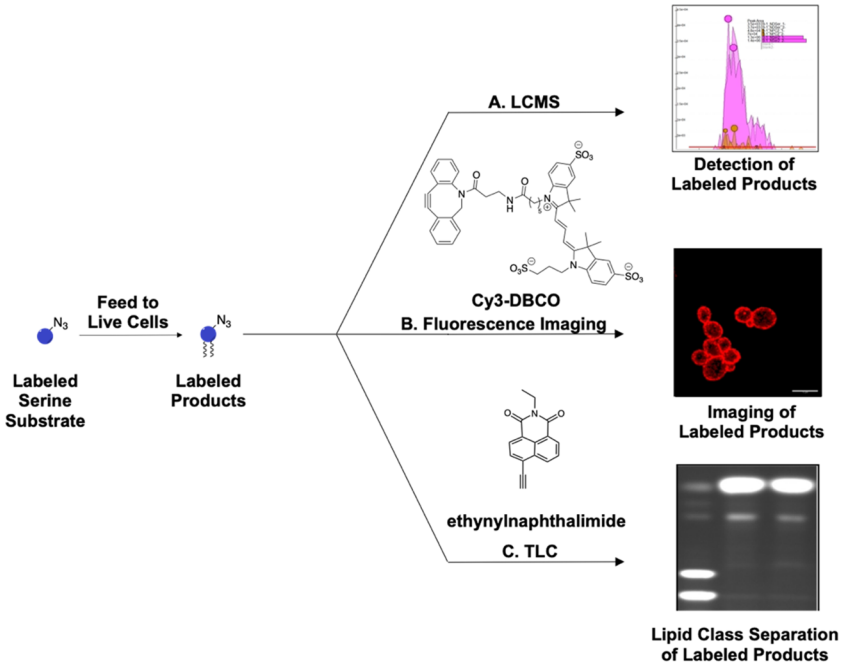

Scheme 2. Synthesis of Clickable Serine Probes N-L-SerN$_3$ and C-L-SerN$_3$ and Structures of Control Probes N-D-SerN$_3$ and C-D-SerN$_3$

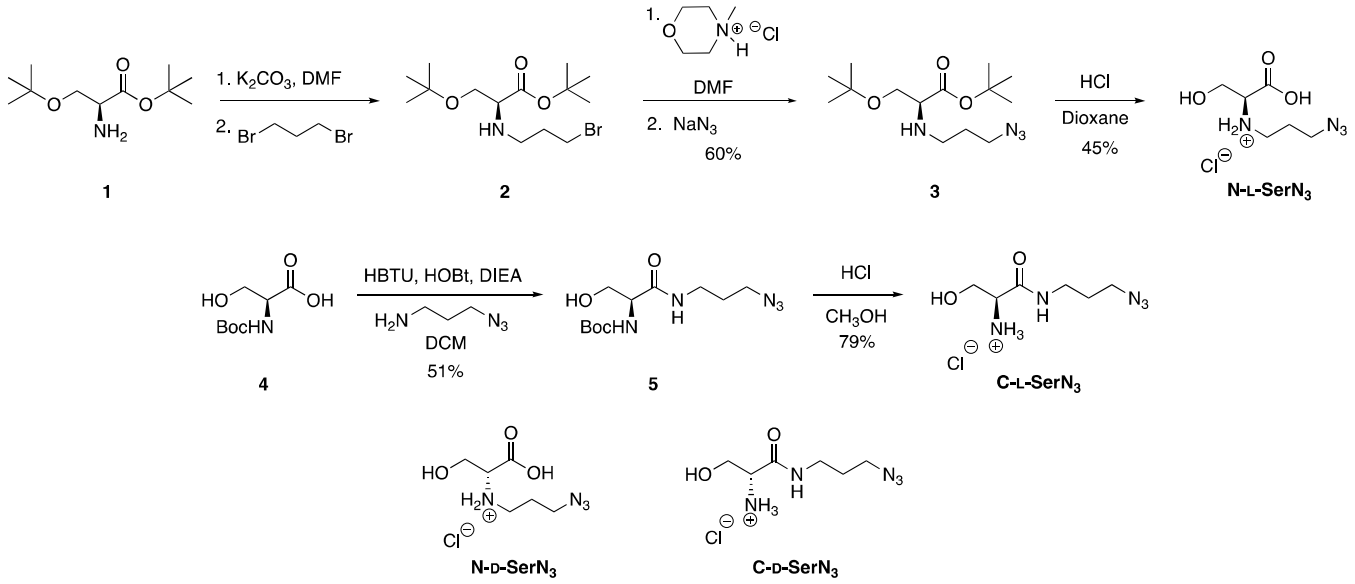

lipidation,[32] important advancements have also enabled the labeling of specific lipid classes, including phospholipids, through the use of tagged headgroup precursors.[33] Related lipids including PC,[34−37] phosphatidic acid (PA),[38−40] glycophosphatidylinositol (GPI) anchors,[41−43] and phosphatidylinositol (PI)[44] have been successfully labeled. However, other important lipid targets, such as PS, have not, to our knowledge, been thus far amenable for the development of bioorthogonal labeling strategies. Herein, we report the metabolic labeling of PS using a series of clickable serine analogues (Scheme 1). We envision that this approach will enhance the ability to track the biosynthesis and localization of PS.

RESULTS AND DISCUSSION

Probe Design and Synthesis. We began by designing tagged analogues of serine since this is the common and direct precursor of PS production. Because the serine side chain hydroxyl group is required for linkage of the headgroup to the glycerolipid scaffold of PS, the remaining carboxyl and amine groups were both pursued as attachment points for the introduction of clickable tags. We focused on azido-serine probes to enable labeling via the strain-promoted azide−alkyne

https://doi.org/10.1021/acschembio.2c00813
ACS Chem. Biol. 2023, 18, 377−384

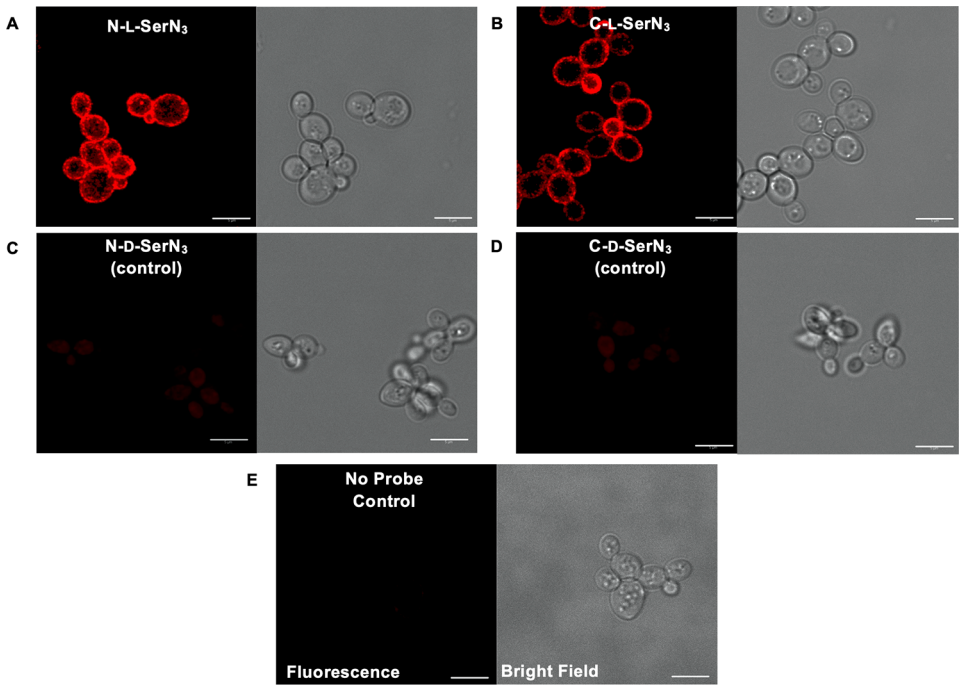

Figure 1. Fluorescence and bright-field microscopy images of *S. cerevisiae* cells grown with **N**-L-**SerN$_3$** (A), **C**-L-**SerN$_3$** (B), **N**-D-**SerN$_3$** (C), **C**-D-**SerN$_3$** (D) (1.5 mM), or negative controls lacking probes (E) harvested at log phase and incubated with **Cy3-DBCO** (1 μM) for fluorescence labeling by SPAAC, which were then fixed. Only cells treated with probes **N**-L-**SerN$_3$** (A) and **C**-L-**SerN$_3$** (B) showed fluorescence (red), which is localized to the cell plasma membrane, with all control cells exhibiting minimal signal. Bright-field images are included to show the locations of cells. Scale bars denote 5 μm.

cycloaddition (SPAAC, copper-free click chemistry) using cyclooctyne-containing reagents. Compound **N**-L-**SerN$_3$** contains a clickable azide tag attached via an azidopropyl moiety appended to the amino group of serine. We envisaged this compound to be a favorable serine mimic since it can retain a positive charge on nitrogen when protonated at neutral pH. This probe was synthesized from *O-tert*-butyl-L-serine *tert*-butyl ester **1** (Scheme 2) through alkylation with 1,3-dibromopropane to bromide **2**, substitution with azide to **3**, and deprotection to **N**-L-**SerN$_3$**. Additionally, we developed probe **C**-L-**SerN$_3$** by instead appending an azidopropyl chain to the C-terminus of serine by forming an amide bond. This probe modifies the charge of serine by removing the carboxylate moiety that prefers the negatively charged state at physiological pH. However, as will be discussed further in subsequent labeling experiments, we hypothesized that probe **C**-L-**SerN$_3$**, when incorporated into labeled PS molecules, may deter further metabolism resulting from decarboxylation into phosphatidylethanolamine (PE). This probe was synthesized from *N*-Boc-serine **4** through amide bond coupling to azidopropanamine to **5** and then Boc deprotection to produce **C**-L-**SerN$_3$**. For both of these probes, enantiomeric versions **N**-D-**SerN$_3$** and **C**-D-**SerN$_3$** were synthesized by the same routes using starting materials with the opposite stereochemistry. It was previously shown by an *in vitro* assay that D-serine does not compete with L-serine as a substrate for the yeast PS synthase enzyme Cho1p until a supracellular concentration of 200 mM D-serine is supplemented, thereby indicating the stringent stereochemical requirements of this enzyme for the natural substrate.[45] Thus, D-serine probes provide valuable negative controls for these studies that are structurally similar to the designed serine substrate analogues.

With these probes prepared, we first sought to determine whether these compounds exhibit a deleterious effect on cell growth. Experiments were performed using *Saccharomyces cerevisiae* cells because they contain significant similarities to mammalian cells in terms of the genes, enzymes, and pathways associated with lipid metabolism[46] and for convenient access to abundant cell samples. Cells were grown in the presence or absence of each probe (1.5 mM), and measurements of optical density at 600 nm (OD_{600}) were used to track optical density over time during cell culture. As can be seen in Figure S2, the resulting growth curves and doubling times for cells that were incubated with **N**-L-**SerN$_3$** or **C**-L-**SerN$_3$** or untreated were very similar, which indicates that these probes do not cause cell toxicity at the concentrations tested. This was quite different from our previous work on PI labeling in which an azido-tagged *myo*-inositol probe yielded deleterious effects on growth.[44] Interestingly, the enantiomeric probes **N**-D-**SerN$_3$** and **C**-D-**SerN$_3$** both resulted in a slight decrease in final cell growth (Figure S2A); however, the doubling time for **C**-D-**SerN$_3$** was significantly different from control (Figure S2B).

Metabolic Labeling of PS in Yeast Cells. We next pursued cellular fluorescence microscopy experiments as an initial step to determine whether these probes enable cellular labeling of PS in *S. cerevisiae* cells (Scheme 1B). In these studies, we imaged products labeled by these probes via SPAAC using dibenzocyclooctyne-Cy3 (**Cy3-DBCO**). Cells were grown in either the presence or absence of probes **N**-L-**SerN$_3$**, **C**-L-**SerN$_3$**, **N**-D-**SerN$_3$**, or **C**-D-**SerN$_3$** and then incubated with the fluorophore **Cy3-DBCO**, washed to remove unbound dye, fixed, and subjected to confocal fluorescence microscopy. As can be observed in Figure 1, both probes **N**-L-**SerN$_3$** and **C**-L-**SerN$_3$** yielded robust fluorescence labeling of cells, while the enantiomeric control

https://doi.org/10.1021/acschembio.2c00813
ACS Chem. Biol. 2023, 18, 377−384

probes **N**-D-**SerN$_3$** and **C**-D-**SerN$_3$** resulted in virtually no signal (Figure 1A–E). Furthermore, the signal resulting from **N**-L-**SerN$_3$** and **C**-L-**SerN$_3$** treatment was observed to be localized at the plasma membranes of these cells (see Figure S3A for inverted black and white images).[47,48] To further analyze the localization of fluorescence, we performed colocalization experiments utilizing CellBright DiD, a known plasma membrane tracer. We observed that fluorescence from both **N**-L-**SerN$_3$** and **C**-L-**SerN$_3$** coincided with DiD signal (Figure S4). We calculated Pearson's correlation coefficients (R) between Cy3 and DiD fluorescence to aid in interpreting the colocalization of the two tracers. The R values corroborated the confocal images wherein the SerN$_3$ probes resulted in a high degree of plasma membrane localization (**N**-L-**SerN$_3$**, R = 0.85; **C**-L-**SerN$_3$**, R = 0.76), while control samples resulted in lower R value (R = 0.31) that likely results in some residual dye being retained in the plasma membrane. The observed signal is in accordance with the known plasma membrane localization of PS in yeast, although PS also resides within the ER (site of phospholipid synthesis) but is only minimally abundant in other organelles.[48,49] We will note that it is possible that particularly prominent localization at the plasma membrane compared with the ER may result from the former being more accessible to the **Cy3-DBCO** dye on the basis of permeability, timing of the experiment, and other conditions. Nevertheless, these results demonstrate that **N**-L-**SerN$_3$** and **C**-L-**SerN$_3$** are effective for cellular labeling and that inversion of the lone stereocenter in each of these compounds abrogates labeling properties. Moreover, these data indicate that our probes allow for stereospecific labeling of cellular membranes.

Because we had observed variations in fluorescence profiles between both sets of L-serine and D-serine probes, we next conducted flow cytometry experiments to quantify differences in fluorescence intensity among these samples. For these experiments, the flow cytometry wavelength options required us to switch to a different clickable dye for labeling. Therefore, we instead employed an AF647-DBCO dye that is active for SPAAC. Flow cytometry analysis of these cell samples (Figure S5) was effective for confirming enhancements in fluorescence for cells labeled by **N**-L-**SerN$_3$** and **C**-L-**SerN$_3$** compared with the enantiomeric probes **N**-D-**SerN$_3$** and **C**-D-**SerN$_3$**.

We observed during **C**-L-**SerN$_3$** labeling experiments that fluorescence signal appeared to be enhanced in budding cells (Figure 2). This is in line with prior work by Grinstein and coworkers, in which detection of PS in *S. cerevisiae* using fluorescently labeled protein (GFP-Lact-C2) exhibited polarized fluorescence at the bud cortex and bud necks of live cells.[50] These results provided additional evidence that labeled molecules from serine probes correlated with known PS localization in support for our belief that this strategy can be used in conjunction with microscopy to track PS in live cells. However, we did not observe enhanced fluorescence labeling in budding cells treated with probe **N**-L-**SerN$_3$** (see, for example, Figure 1A). We speculate that this disparity may result from PS labeled by this probe being diverted to a greater extent into downstream lipid products through decarboxylation into PE and further lipid metabolism. This hypothesis was analyzed through MS experiments that will be discussed below.

PS Probes Are Recognized by the PS Synthase Cho1p. As an initial step to directly evaluate whether these serine probes interact with PS biosynthetic machinery, we assessed their ability to inhibit the activity of PS synthase

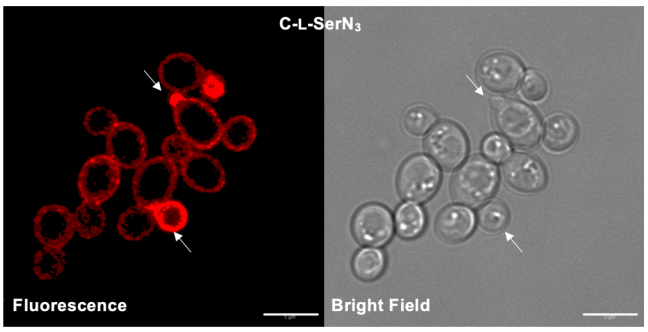

Figure 2. Enhanced labeling of budding cells (labeled with arrows) was observed when *S. cerevisiae* cells were treated with **C**-L-**SerN$_3$**. Persistence of enhanced fluorescence signal at budding sites was observed in 15 ± 4 sets out of 50 randomly selected budding cells. Quantification was performed for 6 biological replicates. Scale bars denote 5 μm.

(Cho1p) from *C. albicans* for the conversion of natural serine to PS. These experiments were performed using *C. albicans* cells because this organism is similar to *S. cerevisiae* in terms of the PS biosynthetic pathway and its PS synthase enzyme (alignment of *Ca*Cho1 and *Sc*Cho1 amino acid sequences in Clustal Omega revealed 60.52% sequence identity), and because we have previously developed a robust assay utilizing cell membrane extracts containing Cho1p to convert tritium-labeled serine (^{3}H-serine) and CDP-DAG into isotopically labeled PS (^{3}H-PS).[45,51,52] These experiments showed that ^{3}H-PS production was diminished by probes **N**-L-**SerN$_3$** and **C**-L-**SerN$_3$** in a dose-dependent manner (Figure 3). Statistical analysis showed that both **N**-L-**SerN$_3$** and **C**-L-**SerN$_3$** displayed significantly decreased enzyme activity for all concentrations tested (1, 5, 10, and 25 mM). It should also be noted that significant inhibition was observed at a probe concentration (1 mM) that is lower than intracellular serine levels (~2 mM).[53] A plausible explanation for this inhibition is that these probes interact with Cho1p in a manner that competes with or blocks conversion of ^{3}H-serine to ^{3}H-PS, thereby providing evidence that these compounds effectively interact with target PS synthase enzymes.

PS Probes Hijack Lipid Metabolic Pathways. We next employed different techniques to determine whether these probes are, in fact, labeling PS. We performed mass-spectrometry-based lipidomics to detect lipid products bearing the added clickable handle (Scheme 1A). We generated lysates from yeast cells (*S. cerevisiae*) grown in the presence or absence of each tagged serine analogue and subjected them to LC/MS. Probe **N**-L-**SerN$_3$** resulted in the detection of azide-tagged products corresponding to PS but also downstream lipids including PE and PC (representative spectra shown in Figure S6A,B and Table S1), which contained the major FAs known to be present in *S. cerevisiae*.[54] Peaks matching expected labeled products were observed in negative mode, with retention times that were comparable with to natural lipid standards. Each of the lipid products that was observed would be expected on the basis of phospholipid biosynthetic transformations (see the pathway substrates marked in brown in Figure S1). Our results support that serine probe **N**-L-**SerN$_3$** is effective as a substrate for conversion to PS, after which it can then undergo decarboxylation to PE derivatives and then methylation to PC analogues. These peaks corresponding to labeled lipids were not observed for control probe **N**-D-**SerN$_3$**, thereby

https://doi.org/10.1021/acschembio.2c00813
ACS Chem. Biol. 2023, 18, 377–384

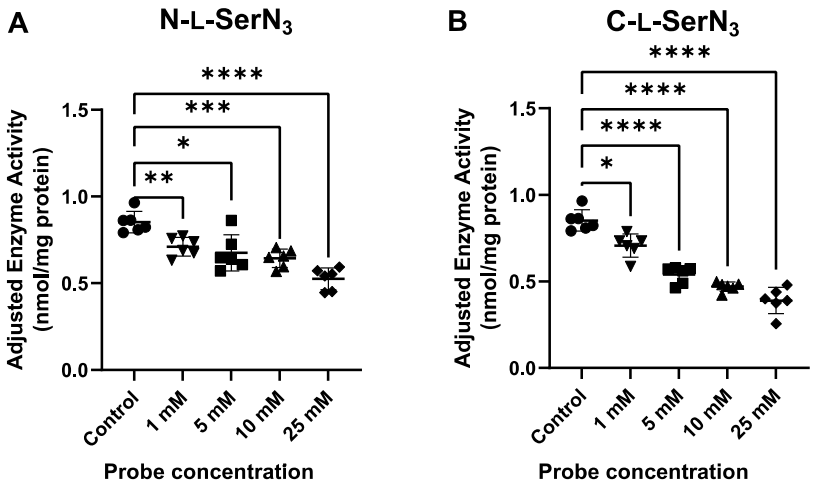

Figure 3. PS synthase activity assays performed using various concentrations (1, 5, 10, and 25 mM) of **N**-L-**SerN**$_3$ (A) or **C**-L-**SerN**$_3$ (B) showed that both of these probes interfere with ^{3}H-serine conversion into PS. All concentrations were compared with control (*, $0.01 < p < 0.05$; **, $0.001 < p < 0.01$; ***, $0.0001 < p < 0.001$; ****, $p < 0.0001$). Statistical analysis was performed using Brown−Forsythe and Welch ANOVA tests. Error bars indicate standard errors for 6 biological replicates.

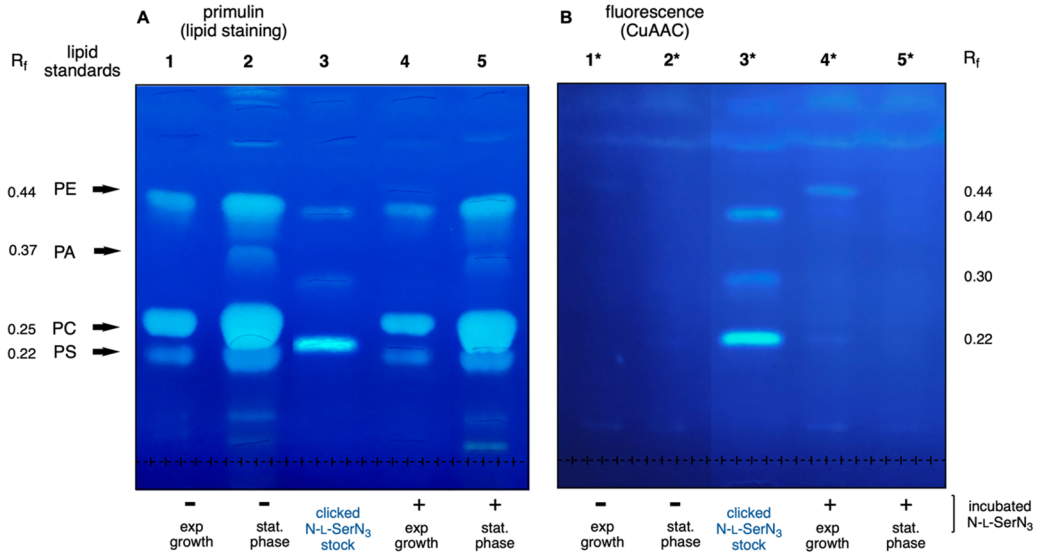

Figure 4. TLC separation of lipids after click-derivatization via CuAAC with fluorogenic ethynylnaphthalimide dye. (A) TLC plate dipped in primulin stain solution to visualize phospholipids (imaged after CuAAC and primulin staining). (B) The same TLC plate as (A) but it displays click-derived fluorescence spots after CuAAC (visualized by fluorescence imaging before primulin staining) and with lanes differentiated by an asterisk. Lanes were loaded with either the unmetabolized **N**-L-**SerN**$_3$ probe (lane 3) or lipid extracts from exponential or stationary growth cells in the absence (lanes 1 and 2, respectively) or presence (lanes 4 and 5, respectively) of **N**-L-**SerN**$_3$. The positions of phospholipid standards PS, PC, PA, and PE are indicated using arrows on the left side of the figure. In lane 4*, two fluorescent click-labeled bands appear close to the commercial standards for PE and PS, while the latter is also close to PC. These click-labeled spots were only detected during exponential growth and not in the stationary phase (lane 5*), which could be because of the time scale of lipid metabolism or alterations in the ratio of PS to other glycerophospholipids since it is known that the total phospholipid composition of yeast cells changes between log and stationary phases.[55] Additionally, the lower click-labeled spot in lane 4* appeared to have a similar R_f value as the click-derived unmetabolized serine probe because of the migration of the PS lipid being dictated by the structure of the amino acid serine. Note that lanes 1−2 and 3−5 were stitched together from two different regions of the same TLC plate images (interior lanes were excised).

further underscoring that inversion of stereochemistry rendered this molecule ineffective for labeling lipids, as suggested by our microscopy studies. Importantly, these data validate that incorporation of the clickable tag at nitrogen does not compromise the normal entry into multiple lipid biosynthetic pathways, although the formation of labeled downstream products is a common challenge for imaging approaches employing metabolic labeling.

We also analyzed **N**-L-**SerN**$_3$-labeled lipid extracts via TLC separation following click derivatization with a fluorogenic ethynylnaphthalimide dye (Scheme 1C). Labeled cells that were harvested during exponential growth (lane 4*) yielded new fluorescence bands, while those obtained from stationary phase (lane 5*) did not (Figure 4B). The most intense fluorescent band from this analysis appears with a retention factor (R_f = 0.44, lane 4*) that overlaps with a commercial standard for PE. There is also a faint band (R_f = 0.22) that overlaps with a commercial standard for PS, although unfortunately, this is also close to the location of the unmetabolized probe (lane 3*) and to the standard for PC

https://doi.org/10.1021/acschembio.2c00813
ACS Chem. Biol. 2023, 18, 377−384

(R_f = 0.25). Nevertheless, these results are in line with the labeled phospholipid peaks that were detected in MS experiments.

We also conducted MS studies using **C-L-SerN$_3$**, which again afforded the production of labeled versions of PS with retention times close to the PS standards that were not observed from enantiomeric control probe **C-D-SerN$_3$** (Table S2, Figure S7). However, as opposed to our prior results with **N-L-SerN$_3$**, cells treated with **C-L-SerN$_3$** did not generate mass peaks corresponding to labeled downstream lipids PE and PC with reasonable retention times on the basis of phospholipid standards. These results are in line with our hypothesis that decarboxylation of labeled PS to PE by Psd1 or Psd2 would be deterred for lipids labeled by **C-L-SerN$_3$** since the carboxyl moiety of this compound has been modified to an amide. We also performed click-tagged TLC experiments using **C-L-SerN$_3$**, (Figure S8). From this experiment, we observed a very faint new fluorescence spot that moved closely with PS standard, although the faintness of this band makes it difficult to draw definitive conclusions. However, we did not observe a higher fluorescent spot in proximity of PE standard, as was observed for TLC analysis using **N-L-SerN$_3$** (Figure 4), which provided further evidence that the labeling of PE is blocked using **C-L-SerN$_3$**. All in all, these results provide evidence that labeling resulting from treatment with **C-L-SerN$_3$** could enable enhanced targeting of PS.

CONCLUSION

These studies support that serine probes **N-L-SerN$_3$** and **C-L-SerN$_3$** act as mimics of this substrate to produce click-tagged PS in yeast cells, as judged by cellular fluorescence labeling, blockage of PS synthase activity, and the detection of labeled products via mass spectrometry and TLC. The probe activities were abrogated simply by inverting the stereochemistry of these compounds using negative controls **N-D-SerN$_3$** or **C-D-SerN$_3$**. Our experiments indicate that PS products resulting from **N-L-SerN$_3$** underwent further modification to produce downstream lipids, such as PE and PC, whereas **C-L-SerN$_3$** appears to show primarily PS labeling among these lipids. To our knowledge, this is the first account of a clickable serine probe for phospholipid labeling, particularly for PS, which is a lipid known to act as a marker on the outer surfaces of diseased cells, such as in cancer. Lipid metabolic labeling in conjunction with fluorescence microscopy using these serine probes will likely provide a useful tool for tracking the biosynthesis and flux of important lipids inside cells. Finally, the distinct lipid labeling patterns from this strategy can be further exploited for the intervention of lipid trafficking and transport mechanisms.

ASSOCIATED CONTENT

Supporting Information

The Supporting Information is available free of charge at https://pubs.acs.org/doi/10.1021/acschembio.2c00813.

Materials and methods, additional figures, synthetic procedures, characterization data for synthetic compounds, flow cytometry data, colocalization studies, mass spectrometry, and TLC results (PDF)

AUTHOR INFORMATION

Corresponding Author

Michael D. Best − *Department of Chemistry, University of Tennessee, Knoxville, Tennessee 37996, United States;* orcid.org/0000-0001-8737-5910; Email: mdbest@utk.edu

Authors

Christelle F. Ancajas − *Department of Chemistry, University of Tennessee, Knoxville, Tennessee 37996, United States*

Shahrina Alam − *Department of Chemistry, University of Tennessee, Knoxville, Tennessee 37996, United States*

Daiane S. Alves − *Department of Biochemistry & Cellular and Molecular Biology, University of Tennessee, Knoxville, Tennessee 37996, United States*

Yue Zhou − *Department of Microbiology, University of Tennessee, Knoxville, Tennessee 37996, United States*

Nicholas M. Wadsworth − *Department of Biochemistry & Cellular and Molecular Biology, University of Tennessee, Knoxville, Tennessee 37996, United States*

Chelsi D. Cassilly − *Department of Microbiology, University of Tennessee, Knoxville, Tennessee 37996, United States*

Tanei J. Ricks − *Department of Chemistry, University of Tennessee, Knoxville, Tennessee 37996, United States*

Adam J. Carr − *Department of Chemistry, University of Tennessee, Knoxville, Tennessee 37996, United States;* orcid.org/0000-0003-4898-8663

Todd B. Reynolds − *Department of Microbiology, University of Tennessee, Knoxville, Tennessee 37996, United States;* orcid.org/0000-0002-2867-7182

Francisco N. Barrera − *Department of Biochemistry & Cellular and Molecular Biology, University of Tennessee, Knoxville, Tennessee 37996, United States;* orcid.org/0000-0002-5200-7891

Complete contact information is available at: https://pubs.acs.org/10.1021/acschembio.2c00813

Notes

The authors declare no competing financial interest.

ACKNOWLEDGMENTS

Research reported in this publication was supported by the National Institute of General Medical Sciences of the National Institutes of Health under award number NIH R15GM120705. The content is solely the responsibility of the authors and does not necessarily represent the official views of the National Institutes of Health. The authors would like to acknowledge the University of Tennessee Advanced Microscopy and Imaging Center, J. Kolape, and J. Dunlap for instrument use and scientific and technical assistance. We also acknowledge S. Campagna, K. Jones, A. Farmer, J. Baccile, and N. Trybala and the UTK Biological and Small Molecule Mass Spectrometry Core for assistance with MS studies.

REFERENCES

(1) Griner, E. M.; Kazanietz, M. G. Protein kinase C and other diacylglycerol effectors in cancer. *Nat. Rev. Cancer* **2007**, *7* (4), 281−294.

(2) Bruntz, R. C.; Lindsley, C. W.; Brown, H. A. Phospholipase D signaling pathways and phosphatidic acid as therapeutic targets in cancer. *Pharmacol. Rev.* **2014**, *66* (4), 1033−1079.

(3) Katso, R.; Okkenhaug, K.; Ahmadi, K.; White, S.; Timms, J.; Waterfield, M. D. Cellular function of phosphoinositide 3-kinases: Implications for development, immunity, homeostasis, and cancer. *Annu. Rev. Cell Dev. Biol.* **2001**, *17*, 615−675.

(4) Mazhab-Jafari, M. T.; Marshall, C. B.; Smith, M. J.; Gasmi-Seabrook, G. M. C.; Stathopulos, P. B.; Inagaki, F.; Kay, L. E.; Neel, B. G.; Ikura, M. Oncogenic and RASopathy-associated K-RAS mutations

relieve membrane-dependent occlusion of the effector-binding site. *Proc. Natl. Acad. Sci. U. S. A.* **2015**, *112* (21), 6625−6630.
(5) Stace, C. L.; Ktistakis, N. T. Phosphatidic acid- and phosphatidylserine-binding proteins. *Biochim. Biophys. Acta* **2006**, *1761* (8), 913−926.
(6) van Genderen, H. O.; Kenis, H.; Hofstra, L.; Narula, J.; Reutelingsperger, C. P. M. Extracellular annexin A5: Functions of phosphatidylserine-binding and two-dimensional crystallization. *Biochim. Biophys. Acta* **2008**, *1783* (6), 953−963.
(7) Andree, H. A. M.; Stuart, M. C. A.; Hermens, W. T.; Reutelingsperger, C. P. M.; Hemker, H. C.; Frederik, P. M.; Willems, G. M. Clustering of Lipid-Bound Annexin-V May Explain Its Anticoagulant Effect. *J. Biol. Chem.* **1992**, *267* (25), 17907−17912.
(8) Cederholm, A.; Frostegard, J. Annexin A5 as a novel player in prevention of atherothrombosis in SLE and in the general population. *Autoimmunity, Pt D* **2007**, *1108*, 96−103.
(9) Rand, J. H.; Wu, X. X.; Quinn, A. S.; Chen, P. J. P.; McCrae, K. R.; Bovill, E. G.; Taatjes, D. J. Human monoclonal antiphospholipid antibodies disrupt the annexin A5 anticoagulant crystal shield on phospholipid bilayers - Evidence from atomic force microscopy and functional assay. *Am. J. Pathol.* **2003**, *163* (3), 1193−1200.
(10) Cederholm, A.; Sul, J.; von Landenberg, P.; Frostegard, J. Annexin A5 in cardiovascular disease and antiphospholipid syndrome: A novel mechanism. *Clin. Exp. Rheumatol.* **2007**, *25* (2), 143−143.
(11) Hanshaw, R. G.; Smith, B. D. New reagents for phosphatidylserine recognition and detection of apoptosis. *Bioorg. Med. Chem.* **2005**, *13* (17), 5035−5042.
(12) Doktorova, M.; Symons, J. L.; Levental, I. Structural and functional consequences of reversible lipid asymmetry in living membranes. *Nat. Chem. Biol.* **2020**, *16* (12), 1321−1330.
(13) Balasubramanian, K.; Schroit, A. J. Aminophospholipid asymmetry: A matter of life and death. *Annu. Rev. Physiol.* **2003**, *65*, 701−734.
(14) Yeung, T.; Gilbert, G. E.; Shi, J.; Silvius, J.; Kapus, A.; Grinstein, S. Membrane phosphatidylserine regulates surface charge and protein localization. *Science* **2008**, *319* (5860), 210−213.
(15) Zwaal, R. F. A.; Comfurius, P.; Bevers, E. M. Surface exposure of phosphatidylserine in pathological cells. *Cell. Mol. Life Sci.* **2005**, *62* (9), 971−988.
(16) Ran, S.; Downes, A.; Thorpe, P. E. Increased exposure of anionic phospholipids on the surface of tumor blood vessels. *Cancer Res.* **2002**, *62* (21), 6132−6140.
(17) Vance, J. Phospholipid synthesis and transport in mammalian cells. *Traffic* **2015**, *16* (1), 1−18.
(18) Billcliff, P. G.; Lowe, M. Inositol lipid phosphatases in membrane trafficking and human disease. *Biochem. J.* **2014**, *461*, 159−175.
(19) Vance, J. E.; Tasseva, G. Formation and function of phosphatidylserine and phosphatidylethanolamine in mammalian cells. *Biochim. Biophys. Acta* **2013**, *1831* (3), 543−554.
(20) Tatsuta, T.; Scharwey, M.; Langer, T. Mitochondrial lipid trafficking. *Trends Cell Biol.* **2014**, *24* (1), 44−52.
(21) Balla, T. Phosphoinositides: Tiny lipids with giant impact on cell regulation. *Physiol. Rev.* **2013**, *93* (3), 1019−1137.
(22) Di Paolo, G.; De Camilli, P. Phosphoinositides in cell regulation and membrane dynamics. *Nature* **2006**, *443* (7112), 651−657.
(23) Frasch, S. C.; Bratton, D. L. Emerging roles for lysophosphatidylserine in resolution of inflammation. *Prog. Lipid Res.* **2012**, *51* (3), 199−207.
(24) Sletten, E. M.; Bertozzi, C. R. Bioorthogonal chemistry: fishing for selectivity in a sea of functionality. *Angew. Chem., Int. Ed. Engl.* **2009**, *48* (38), 6974−98.
(25) Best, M. D. Click chemistry and bioorthogonal reactions: unprecedented selectivity in the labeling of biological molecules. *Biochemistry* **2009**, *48* (28), 6571−6584.
(26) Saxon, E.; Bertozzi, C. R. Cell surface engineering by a modified Staudinger reaction. *Science* **2000**, *287* (5460), 2007−2010.
(27) Baskin, J. M.; Bertozzi, C. R. Bioorthogonal click chemistry: Covalent labeling in living systems. *QSAR Comb. Sci.* **2007**, *26* (11−12), 1211−1219.
(28) Hanson, S. R.; Greenberg, W. A.; Wong, C. H. Probing glycans with the copper(I)-catalyzed [3 + 2] azide-alkyne cycloaddition. *QSAR Comb. Sci.* **2007**, *26* (11−12), 1243−1252.
(29) Laughlin, S. T.; Bertozzi, C. R. Imaging the glycome. *Proc. Natl. Acad. Sci. U. S. A.* **2009**, *106* (1), 12−17.
(30) Sletten, E. M.; Bertozzi, C. R. Bioorthogonal chemistry: Fishing for selectivity in a sea of functionality. *Angew. Chem., Int. Ed.* **2009**, *48* (38), 6974−6998.
(31) Thiele, C.; Papan, C.; Hoelper, D.; Kusserow, K.; Gaebler, A.; Schoene, M.; Piotrowitz, K.; Lohmann, D.; Spandl, J.; Stevanovic, A.; Shevchenko, A.; Kuerschner, L. Tracing Fatty Acid Metabolism by Click Chemistry. *ACS Chem. Biol.* **2012**, *7* (12), 2004−2011.
(32) Hang, H. C.; Wilson, J. P.; Charron, G. Bioorthogonal chemical reporters for analyzing protein lipidation and lipid trafficking. *Acc. Chem. Res.* **2011**, *44*, 699−708.
(33) Ancajas, C. F.; Ricks, T. J.; Best, M. D. Metabolic labeling of glycerophospholipids via clickable analogs derivatized at the lipid headgroup. *Chem. Phys. Lipids* **2020**, *232*, 104971.
(34) Jao, C. Y.; Roth, M.; Welti, R.; Salic, A. Biosynthetic labeling and two-color imaging of phospholipids in cells. *Chembiochem* **2015**, *16* (3), 472−476.
(35) Iyoshi, S.; Cheng, J. L.; Tatematsu, T.; Takatori, S.; Taki, M.; Yamamoto, Y.; Salic, A.; Fujimoto, T. Asymmetrical distribution of choline phospholipids revealed by click chemistry and freeze-fracture electron microscopy. *ACS Chem. Biol.* **2014**, *9* (10), 2217−2222.
(36) Jao, C. Y.; Roth, M.; Welti, R.; Salic, A. Metabolic labeling and direct imaging of choline phospholipids in vivo. *Proc. Natl. Acad. Sci. U. S. A.* **2009**, *106* (36), 15332−15337.
(37) Wang, D.; Du, S.; Cazenave-Gassiot, A.; Ge, J.; Lee, J. S.; Wenk, M. R.; Yao, S. Q. Global Mapping of Protein-Lipid Interactions by Using Modified Choline-Containing Phospholipids Metabolically Synthesized in Live Cells. *Angew. Chem., Int. Ed. Engl.* **2017**, *56* (21), 5829−5833.
(38) Bumpus, T. W.; Baskin, J. M. A Chemoenzymatic Strategy for Imaging Cellular Phosphatidic Acid Synthesis. *Angew. Chem., Int. Ed. Engl.* **2016**, *55* (42), 13155−13158.
(39) Bumpus, T. W.; Baskin, J. M. Clickable Substrate Mimics Enable Imaging of Phospholipase D Activity. *ACS Cent. Sci.* **2017**, *3* (10), 1070−1077.
(40) Liang, D. J.; Wu, K. N.; Tei, R.; Bumpus, T. W.; Ye, J.; Baskin, J. M. A real-time, click chemistry imaging approach reveals stimulus-specific subcellular locations of phospholipase D activity. *Proc. Natl. Acad. Sci., U.S.A.* **2019**, *116* (31), 15453−15462.
(41) Lu, L. L.; Gao, J.; Guo, Z. W. Labeling cell surface GPIs and GPI-anchored proteins through metabolic engineering with artificial inositol derivatives. *Angew. Chem., Int. Ed.* **2015**, *54* (33), 9679−9682.
(42) Jaiswal, M.; Zhu, S.; Jiang, W.; Guo, Z. Synthesis and evaluation of N(α),N(ε)-diacetyl-l-lysine-inositol conjugates as cancer-selective probes for metabolic engineering of GPIs and GPI-anchored proteins. *Org. Biomol Chem.* **2020**, *18* (15), 2938−2948.
(43) Craig, K. C.; Guo, Z. Design and synthesis of 4-azido-phosphatidylinositol as a potential probe for metabolic engineering of glycosylphosphatidylinositol on cells. *Journal of Carbohydrate Chemistry* **2022**, *41*, 238−248.
(44) Ricks, T. J.; Cassilly, C. D.; Carr, A. J.; Alves, D. S.; Alam, S.; Tscherch, K.; Yokley, T. W.; Workman, C. E.; Morrell-Falvey, J. L.; Barrera, F. N.; Reynolds, T. B.; Best, M. D. Labeling of Phosphatidylinositol Lipid Products in Cells through Metabolic Engineering by Using a Clickable myo-Inositol Probe. *Chembiochem* **2019**, *20* (2), 172−180.
(45) Cassilly, C. D.; Farmer, A. T.; Montedonico, A. E.; Smith, T. K.; Campagna, S. R.; Reynolds, T. B. Role of phosphatidylserine synthase in shaping the phospholipidome of Candida albicans. *FEMS Yeast Res.* **2017**, *17* (2), fox007.

https://doi.org/10.1021/acschembio.2c00813
ACS Chem. Biol. 2023, 18, 377−384

(46) Henry, S. A.; Kohlwein, S. D.; Carman, G. M. Metabolism and regulation of glycerolipids in the yeast saccharomyces cerevisiae. *Genetics* **2012**, *190* (2), 317−349.
(47) Zinser, E.; Sperka-Gottlieb, C. D.; Fasch, E. V.; Kohlwein, S. D.; Paltauf, F.; Daum, G. Phospholipid synthesis and lipid composition of subcellular membranes in the unicellular eukaryote Saccharomyces cerevisiae. *J. Bacteriol.* **1991**, *173* (6), 2026−34.
(48) van Meer, G.; Voelker, D. R.; Feigenson, G. W. Membrane lipids: where they are and how they behave. *Nat. Rev. Mol. Cell Biol.* **2008**, *9* (2), 112−124.
(49) Klug, L.; Daum, G. Yeast lipid metabolism at a glance. *FEMS Yeast Research* **2014**, *14* (3), 369−388.
(50) Fairn, G. D.; Hermansson, M.; Somerharju, P.; Grinstein, S. Phosphatidylserine is polarized and required for proper Cdc42 localization and for development of cell polarity. *Nat. Cell Biol.* **2011**, *13* (12), 1424−1430.
(51) Chen, Y. L.; Montedonico, A. E.; Kauffman, S.; Dunlap, J. R.; Menn, F. M.; Reynolds, T. B. Phosphatidylserine synthase and phosphatidylserine decarboxylase are essential for cell wall integrity and virulence in Candida albicans. *Mol. Microbiol.* **2010**, *75* (5), 1112−32.
(52) Zhou, Y.; Cassilly, C. D.; Reynolds, T. B. Mapping the Substrate-Binding Sites in the Phosphatidylserine Synthase in Candida albicans. *Front. Cell. Infect. Microbiol.* **2021**, *11* (1281), 765266.
(53) Hans, M. A.; Heinzle, E.; Wittmann, C. Free intracellular amino acid pools during autonomous oscillations in Saccharomyces cerevisiae. *Biotechnol. Bioeng.* **2003**, *82* (2), 143−51.
(54) Tuller, G.; Nemec, T.; Hrastnik, C.; Daum, G. Lipid composition of subcellular membranes of an FY1679-derived haploid yeast wild-type strain grown on different carbon sources. *Yeast* **1999**, *15* (14), 1555−64.
(55) Cottrell, S. F.; Getz, G. S.; Rabinowitz, M. Phospholipid accumulation during the cell cycle in synchronous cultures of the yeast, Saccharomyces cerevisiae. *J. Biol. Chem.* **1981**, *256* (21), 10973−10978.

https://doi.org/10.1021/acschembio.2c00813
ACS Chem. Biol. 2023, 18, 377−384